RSC Advances

PAPER

View Article Online
View Journal | View Issue

Cite this: *RSC Adv.*, 2025, **15**, 24566

A short amphipathic peptide-based injectable hydrogel with antibacterial properties†

Dorien Aerssens,[a] Atiruj Theppawong,[a] Hue Vu,[a] Petra Rigole,[b] Marleen Van Troys,[c] Tom Coenye,[b] Richard Hoogenboom,[d] Steven Ballet,[e] Charlotte Martin[e] and Annemieke Madder *[a]

Received 17th May 2025
Accepted 26th June 2025

DOI: 10.1039/d5ra03481g

rsc.li/rsc-advances

Hydrogel materials have gained considerable interest to be used as aids in the healing of chronic and traumatic wounds, in view of their tunable mechanical stability, biocompatibility and biodegradability. Here, we describe the development of a new injectable and antibacterial peptide-based hydrogel that is composed of only nine natural amino acids. By covalently merging a short antibacterial peptide sequence with a short hydrogelator peptide sequence, the biologically active sequence H-RWRWQFQFK-NH_2 was prepared, which self-assembled into a thixotropic hydrogel, a so-called 'biogel'. This biogel and a related co-formulation of the short antimicrobial peptide H-RWRW-NH_2 with the hydrogelating hexamer H-FQFQFK-NH_2 were evaluated as potential wound dressings by means of an *in vitro* wound model using *S. aureus*, *A. baumannii* or *P. aeruginosa*. The obtained data showed that both the biogel and the co-formulation strategy appeared to be particularly effective towards *A. baumannii* and *P. aeruginosa*.

Introduction

Wounds are injuries to the skin and underlying tissues that in the majority of cases occur as a result of trauma or surgery. When open wounds are not treated properly, pathogenic bacteria can grow inside these wounds and potentially migrate into the blood circulatory system, resulting in systemic infections. While antibiotics have become the standard treatment of infections and have certainly played an important role in therapy, overuse and misuse of antibiotics has led to the development of antibiotic-resistant organisms.[1] In addition, also the common use of medical devices and implants is associated with a significant risk of biofilm-associated infections and it is estimated that 80% of chronic infections are due to biofilm formation on the surfaces of applied medical materials, including catheters, cardiac implants, vascular and orthopedic prostheses, and others.[2] Therefore, effective therapeutic strategies are needed that not only promote healing, but at the same time prevent infection as well.[3]

Applying moist saline gauze over a wound bed represents a widely accepted wet-to-dry wound dressing that has been a gold standard within the context of wound healing. However, replacement of such dressings requires removal of the dried gauze and commonly damages the healing wound, which can be traumatic and painful for patients.[4,5] Keeping the wound moistured is thus of utmost importance to increase patient compliance and hydrogels offer particularly interesting properties in that context, as they are highly hydrated materials. More specifically, hydrogel materials that display antibacterial activity have gained a lot of interest to be used as aids in the healing of chronic and traumatic wounds, since they are not only able to provide a more moist environment, but at the same time address the infection.[6,7]

Generally, the antimicrobial agent is encapsulated within the hydrogel and released over a period of time (encapsulation and release of the active agent is hereafter referred to as a co-formulation strategy).[8] In this context, multiple examples of hydrogels co-formulated with silver ions or nanoparticles have been reported.[9–11] Alternatively, the antimicrobial agent can be covalently linked to a hydrogel scaffold.[12]

Among the various utilized hydrogelating materials, peptide-based hydrogels attract much attention due to their high water content, but also their tunable mechanical stability, biocompatibility and biodegradability, as well as excellent injectability.[13] Within the field of inherently antibacterial peptide hydrogels, multiple peptide derivatives have been reported and

[a]*Organic and Biomimetic Chemistry Research Group, Department of Organic and Macromolecular Chemistry, Ghent University, 9000 Ghent, Belgium. E-mail: annemieke.madder@ugent.be*

[b]*Department of Pharmaceutical Analysis, Ghent University, 9000 Ghent, Belgium*

[c]*Department of Biomolecular Medicine, Ghent University, 9000 Ghent, Belgium*

[d]*Supramolecular Chemistry Group, Centre of Macromolecular Chemistry (CMaC), Department of Organic and Macromolecular Chemistry, Ghent University, 9000 Ghent, Belgium*

[e]*Research Group of Organic Chemistry, Vrije Universiteit Brussel, B-1050 Brussels, Belgium*

† Electronic supplementary information (ESI) available. See DOI: https://doi.org/10.1039/d5ra03481g

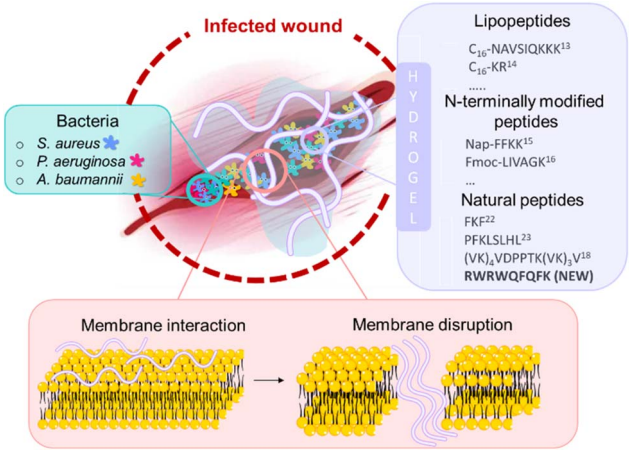

Fig. 1 Schematic overview of how an infected wound can be treated with an antibacterial peptide-based hydrogel (purple box) to improve wound healing. The proposed mechanism of action is illustrated in the red box, and the type of bacteria considered in this study are detailed in the green box.

they can be divided into several categories, depending on the type of peptide hydrogelator used (Fig. 1). A first category encompasses lipopeptides such as C16-KR-NH_2 and C16-NAVSIQKKK-NH_2, which were reported to show bactericidal properties against both Gram-positive and Gram-negative bacteria.[14,15] These lipopeptides are designed to mimic the features of antimicrobial peptides (AMPs), *i.e.* positive net charge and amphipathicity. The positively charged KR or KKK fragments are able to interact with the negatively charged membrane of bacteria, while the hydrophobic lipid tail can insert itself into their membrane, resulting in the formation of pores in the bacterial cell membrane, ultimately killing the bacteria.[13]

The second category of antibacterial peptide hydrogelators consists of N-terminally protected peptides including Fmoc-LIVAGK-NH_2,[16] Nap-FFKK-OH,[17] Ac-K^{D}H^{D}H^{D}Q^{D}K^{D}L^{D}V^{D}F^{D}F^{D}A^{D}K^D-NH_2,[18] and Fmoc-WWRR-NH_2,[19] which all have been reported to exhibit significant antibacterial activity. A similar mode of action as for lipopeptides has been suggested.[16,17,20]

Finally, the third category of self-assembling peptides is entirely composed of natural L or D-amino acids. For example, the β-hairpin MAX1 (H-VKVKVKVKV^{D}PPTKVKVKVKV-NH_2), developed by Schneider *et al.* to be used as a drug delivery vehicle and for regenerative tissue applications,[21,22] appeared to have inherent antibacterial properties.[23] Upon contact with the surface of MAX1 hydrogels, different types of drug-susceptible Gram-positive and Gram-negative bacteria were killed. In order to design a hydrogel system that is able to also kill drug-resistant bacteria, the amino acid composition of the hydrophilic face of the MAX1 β-hairpin was fine-tuned by replacing the *K* residue at position 6 and 17 with an *R* residue, resulting in the MARG1 peptide (H-VKVKVRVKV^{D}PPTKVKVRVKV-NH_2) peptide.[24] By making use of confocal microscopy and a surface of tissue culture treated polystyrene, Schneider and colleagues were able to demonstrate (i) that MARG1-based hydrogels inhibit bacterial proliferation and (ii) that upon contact with the hydrogel surface the *Staphylococcus aureus* bacteria die. Though the authors do not describe the exact mechanism of action, it was hypothesized that membrane disruption takes place due to the cationic nature of these peptides.[24] As the parent peptide is of considerable length and contains D-amino acids the quest for shorter and simpler systems based solely on L-amino acids remained.

The shortest possible hydrogelator with inherent antibacterial properties that is reported in literature, is the amphipathic β-sheet forming H-FKF-OH peptide.[25] This antibacterial H-FKF-OH hydrogel was evaluated in a rat skin lesion model. Though it was able to reduce the bacterial cell count of *Pseudomonas aeruginosa*, application of the H-FKF-OH hydrogel did not improve wound closure compared to untreated wounds. Noticeably, the H-FKF-OH peptide only showed antimicrobial properties in its self-assembled state. Once the peptide was released in solution, no antimicrobial effect could be demonstrated, making this only effective as contact antibacterial agent. More recently, a slightly longer gelating peptide, referred to as Jelleine-1 (H-PFKLSLHL-NH_2), was shown to possess antibacterial properties, as reported by Zhou *et al.*[26] The same authors further showed that Jelleine-1 hydrogels could promote wound healing in a burn wound infected with methicillin-resistant *S. aureus* (MRSA).

Given our recent work in the development of an amphipathic hexapeptide-based hydrogelator platform,[27–31] for which we previously reported applications in the context of painkilling,[28] we decided to explore the potential of this platform for the design of short, inherently antibacterial hydrogels composed of only natural amino acids. For that purpose, we aimed at attaching a short (non-gelating) antibacterial peptide to our previously developed H-FQFQFK-NH_2 hydrogelator sequence. In order to make the final peptide constructs as short as possible, we searched for ultrashort antibacterial peptide sequences. Since the earlier mentioned H-FKF-OH peptide only displays antibacterial properties in its self-assembled state,[25] literature was screened for short natural amino acid containing peptides that also display antibacterial properties in solution.

The shortest peptide reported that meets this criterion is a hexapeptide composed of only *R* and *W* residues, the H-RWRWRW-NH_2 peptide.[32,33] In 2006, Liu *et al.* were able to show that even shorter tetrapeptide versions thereof retained antibacterial properties when covalently linking large numbers of the monomeric antimicrobial tetrapeptides to a polymaleic anhydride (PMA) chain. While PMA has no inherent antibacterial properties, Liu *et al.* were able to demonstrate that the resulting material was characterized by a 10-fold improvement in MIC_{50} value compared to the tetrapeptides in solution.[34] Very recently, Valéry *et al.* not only demonstrated the antimicrobial propensity of Fmoc-WWRR-NH_2 in solution, but also studied the self-assembly process that results in soft Fmoc-WWRR-NH_2 based hydrogels ($G' \sim 100$ Pa).[19]

Here, we explored the combination of an unprotected version of these short tetrapeptides with our short hydrogelating peptides to obtain injectable hydrogel formulations that are solely based on natural amino acids. Next to the

covalently linked hydrogel materials embedding different combinations of RW tetrapeptides, we also studied co-formulations in which the same antimicrobial peptide is encapsulated within a matrix of the parent **H-FQFQFK-NH$_2$** peptide. Hence, this work provides a new strategy for the design and synthesis of new injectable antimicrobial peptide hydrogels.

Materials and methods

Peptide synthesis

Peptides were synthesized using the Fmoc-based solid-phase peptide synthesis (SPPS) strategy, either manually or using a SYRO Multiple Peptide Synthesizer (Multisyntech) or a Multi-Pep RSi (Intavis). Rink amide AM resin (100–200 mesh, 0.92 mmol g^{-1}) was used as solid support, enabling the synthesis of C-terminal peptide amides. Amino acids (4 equiv.) were coupled with *O*-(benzotriazole-1-yl)-*N*,*N*,*N*′,*N*′-tetramethyluronium hexafluoro-phosphate (HBTU, 4 equiv.) and *N*,*N*-diisopropylethylamine (DIPEA, 8 equiv.), in dimethylformamide (DMF). Deprotection of the Fmoc-group was conducted before amino acid coupling, using a solution of piperidine in DMF (40 : 60% v/v). All washing steps were performed with DMF followed by then dichloromethane (DCM). After synthesis, the peptides were cleaved from the solid support while simultaneously achieving side chain deprotection, by treatment with a mixture of trifluoroacetic acid (TFA), triisopropylsilane (TIS) and H_2O (95 : 2.5 : 2.5% v/v/v), for 2 h at RT. The cleavage solution was evaporated under reduced pressure and the crude mixture dissolved using a solution of acetonitrile (ACN) and H_2O (50 : 50% v/v). Subsequently, the peptides were purified by preparative reversed phase high-performance liquid chromatography (RP-HPLC) (see ESI†).

Hydrogel preparation

Gelation was achieved by adding PBS solution (with or without cargo) to a 1.5 mL Eppendorf tube containing the peptide hydrogelator (acetate salt). The tubes were then repetitively vortexed (1 min) and sonicated (5 min), after which they were left to rest overnight at room temperature. The final peptide concentration is 1–2 w/v% depending on the formulation.

Circular dichroism

For this experiment, an AVIV Model 410 instrument (Biomedical Inc., Lakewood, NJ USA) was used. The CD spectra were recorded at 25 °C. The peptide concentration was 500 μg mL^{-1} in phosphate buffer (75 mM Na_2HPO_4, 25 mM NaH_2PO_4, pH 7.11). The spectra were recorded at 100 nm min^{-1} scan rate and a bandwidth of 1 nm in a wavelength range of 190–260 nm using a cell of 1 mm path length.

Thioflavin T fluorescence assay

Peptide samples were prepared in phosphate buffered saline (PBS) and incubated for 1 hour. 2 μL of the 10 mM stock solution of thioflavin T (ThT) in water was added to 400 μL of each peptide sample to obtain a final ThT concentration of 50 μM. The mixtures were incubated for 5 min before each measurement. The fluorescence signal from 460–600 nm was recorded with a Varian Cary Eclipse Fluorescence Spectrophotometer at excitation wavelength of 440 nm, excitation slit width 10 nm and emission slit width 10 nm. The spectra were corrected by subtracting the fluorescence signal of a blank (no peptide) containing 50 μM ThT in PBS.

Rheology

For the rheology measurements, an Anton Paar Physica MCR 301 rheometer was used. The results were analysed with Rheoplus software. The shear recovery experiments were performed on 350 μL of hydrogel. The hydrogel was loaded on a 25 mm plate. After injection of the sample, the sample was allowed to rest for 5 minutes, prior to starting the measurement. For the shear recovery experiment, the G' and G'' were first measured for 60 seconds at a frequency of 1 Hz and a shear strain (γ) of 1%. Subsequently, the γ was increased to 50% for 30 seconds. This cycle was repeated 4 times in each experiment. The measurements were performed in threefold applying a normal force of 1 N onto the sample at a temperature of 25 °C.

In vitro release experiment

The *in vitro* release behavior of antimicrobial peptides and peptide hydrogelators from the hydrogels was evaluated by determining the cumulative release value at each timepoint and the cumulative release curve was drawn as the function of time. Briefly, 100 μL of each hydrogel was prepared as described above in an Eppendorf tube (1.5 mL). At the start of the release experiment, 500 μL of a PBS 1× solution (10 mM, pH 7.4) was carefully added on top of each gel (= timepoint 0). At regular timepoints, the supernatant was homogenized and aliquots of 10 μL were collected and replaced by equal amounts of fresh PBS. Subsequently, these samples were analyzed with reversed phase high-performance liquid chromatography (RP-HPLC) (see ESI†), where the area under the curve (AUC) value was determined for each sample. Hence, the cumulative doses released (M_t) could be calculated by making use of a calibration curve. Finally, the cumulative cargo release percentage was determined over time, considering the initial encapsulated dose (M_i), using eqn (1).

$$\%\text{cumulative cargo release} = M_t/M_i \times 100 \quad (1)$$

In vitro wound model

The artificial dermis (AD) samples (for details see ESI†) were placed in the wells of a 24-well microtiter plate (TPP). 500 μL of Bolton Broth with 50% plasma (Sigma-Aldrich) and 5% freeze–thaw laked horse blood was added on the AD (and was entirely taken up by the AD) and 500 μL of this medium was added around the AD to avoid dehydration during the experiment. An overnight culture of the tested bacterial strain (*S. aureus* Mu50, *A. baumannii* NCTC13423 or *P. aeruginosa* PAO1) was pelleted, washed, and resuspended in physiological saline (PS), and subsequently diluted to 10^6 CFU mL^{-1}. Ten microliter aliquots

of the cell suspension were spotted on each AD. To evaluate the antibacterial activity of the hydrogels, the hydrogel was placed over each AD 4 hours after inoculation, and subsequently the plate was incubated for 24 hours at 37 °C. For quantification by plating, AD were placed into tubes containing 10 mL PS, the sessile cells were removed from the AD by three cycles of vortexing (30 s) and sonication (30 s; Branson 3510; Branson Ultrasonics Corp., Danbury, CT) and the number of CFU per biofilm was determined by plating the resulting suspensions. Further information can be found in the ESI.†

Result and discussion

Biogel design

The short antibacterial sequence **H-RWRW-NH$_2$** was merged with our previously designed **H-FQFQFK-NH$_2$** peptide by the mere N-terminal extension of the parent hexamer hydrogelator sequence (see Table 1, **P1**). Additionally, inspired by the work reported by Liu *et al.*,[34] we also considered variations of the resulting peptides, resulting in the biogelator sequences **P1**, **P2** and **P3**. Simultaneously, in an attempt to shorten the sequences as much as possible, we further investigated whether the first phenylalanine of the parent hydrogelator sequence **H-FQFQFK-NH$_2$** could be left out without compromising gelation (cfr. biogelators **P4** and **P5**).

For each peptide sequence, 1 or 2 mg (cfr. Table 1) of peptide material was dissolved in 100 μL PBS and the gelation behavior was evaluated *via* the inverted tube test. As can be seen from Tables 1 and SI1,† peptides **P1**, **P3** and **P4** formed stable hydrogels at 2 w/v%. For peptides **P2** and **P5**, only viscous solutions were observed at this concentration. However, co-formulation of 1 w/v% of each sequence with 1 w/v% of the **H-FQFQFK-NH$_2$** parent peptide nicely resulted in self-supporting hydrogels. All peptides were then evaluated in a preliminary antibacterial screening assay. For this purpose, a stock solution of 4 mg mL^{-1} in MQ water was made of each peptide. The minimal bactericidal concentration (MBC) and minimum inhibitory concentration (MIC) values for all aforementioned biogels were obtained for a series of bacterial strains, including *S. aureus* (ATCC 25923), *B. subtilis*, *P. aeruginosa* and *A. baumannii* (see Fig. 2 and SI9†). Inspection of the data shown in Fig. 2 revealed that the lowest overall MBC values for the four bacterial strains were consistently obtained for peptides **P4** and **P5**. As only peptide **P4** was gelating on its own, under the standard conditions (*i.e.* without addition of the parent hydrogelator sequence), it was selected for further evaluation and compared to a co-formulation of the parent antibacterial peptide, *i.e.* H-RWRW-NH$_2$ (**RWRW**) embedded in the parent **H-FQFQFK-NH$_2$** hydrogel.

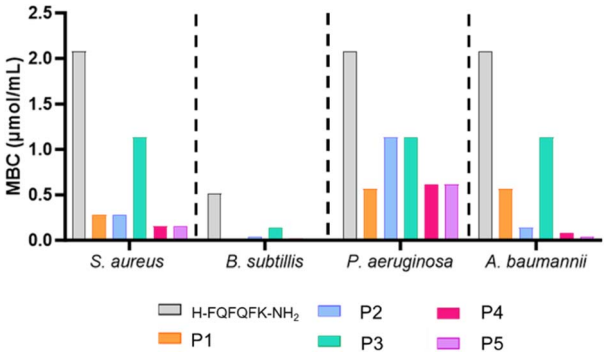

Fig. 2 Minimum bactericidal concentration (MBC) values (μmol mL^{-1}) for Gram-positive (*S. aureus* and *B. subtillis*) and Gram-negative (*P. aeruginosa*, *A. baumannii*) bacteria for all biogelators **P1** (orange), **P2** (blue), **P3** (green), **P4** (pink), and **P5** (purple) and **H-FQFQFK-NH$_2$** (grey). This screening experiment was performed once.

Biogel characterization

The secondary structures and the self-assembly process of the parent peptide **H-FQFQFK-NH$_2$** have been extensively examined and thoroughly discussed before. It was revealed that, at sufficiently high concentration, β-sheets are the most abundant secondary structure elements and constitute the fundamental building block for fiber formation.[35] It was also reported earlier by Ballet and coworkers that adding the RGD tripeptide to the original hexamer sequence disturbed the alternating hydrophilic-hydrophobic amino acid pattern and increased the solubility of the peptide, therefore reducing the β-sheet propensity as well as fiber formation, and ultimately resulting in a weaker hydrogel network.[35] In case of the **P4** peptide however, as the even spacing of hydrophilic groups is preserved, it is expected that the peptide's self-assembly into β-sheet structures is maintained. However, while P4 formed a stable hydrogel, due to significant interference of the tryptophan residues,[36] it was difficult to determine the assembly state *via* circular dichroism (CD) measurements.

Table 1 Overview of all peptide sequences, their gelation properties and the pH of the corresponding biogel formulation. For each peptide in this table, the acetate salt was used and three repeat experiments were carried to determine the pH

Biogelator sequences (BS)	Optimal hydrogen formulation	pH
H-RWRWFQFQFK-NH$_2$ (**P1**)	2 w/v% **BS**	6.52 ± 0.15
H-WRWRFQFQFK-NH$_2$ (**P2**)	1 w/v% **BS** + 1 w/v% H-FQFQFK-NH$_2$	6.40 ± 0.20
H-RRWWFQFQFK-NH$_2$ (**P3**)	2 w/v% **BS**	6.31 ± 0.13
H-RWRWQFQFK-NH$_2$ (**P4**)	2 w/v% **BS**	6.23 ± 0.14
H-RRWWQFQFK-NH$_2$ (**P5**)	1 w/v% BS + 1 w/v% H-FQFQFK-NH$_2$	6.29 ± 0.21

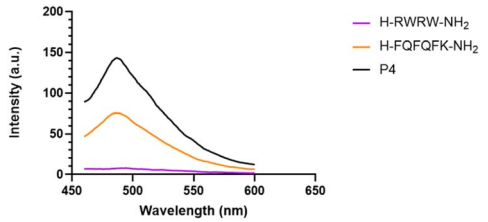

Fig. 3 Fluorescence spectra of ThT upon incubation with **P4** at 1 w/v% (black), **H-FQFQFK-NH$_2$** at 1 w/v% (orange), and **H-RWRW-NH$_2$** at 0.55 w/v% (purple). All peptides were prepared in PBS (pH 7.4).

Therefore, a thioflavin T (ThT) fluorescence assay was employed to verify the secondary structure of the assembled peptides. As can be seen in Fig. 3, for both **H-FQFQFK-NH$_2$** and **P4** an intense fluorescent peak at 485 nm was obtained, suggesting the existence of the β-sheet fibrils in the samples of both peptides. This was not observed in the case of the antibacterial sequence H-RWRW-NH$_2$. Furthermore, after subtracting the background fluorescence of the peptides, **P4** and **H-FQFQFK-NH$_2$** showed comparable ThT fluorescence intensity, suggesting a similar degree of fibrillization (Fig. SI11†).

Next, in order to study the stiffness and the shear thinning properties of the biogel **P4** and compare them to those of the co-formulated gel, rheological analyses were performed. In Fig. 4, the mechanical properties (G' and G'') of the **P4** biogel (pink), the **H-FQFQFK-NH$_2$** hydrogel (blue) and the co-formulated **H-RWRW-NH$_2$** within **H-FQFQFK-NH$_2$** hydrogel (orange) are represented. The dark colors show the G', whereas the lighter colors correspond to G'' and it can be noticed that the G' values are generally larger than the G'' values for all tested systems, indicating that the analyzed sample behaves as a viscoelastic solid. This confirms that a hydrogel was obtained through physical crosslinking of, presumably, peptide nanofibers.[37] The G' of each tested hydrogel system was higher than 1000 Pa, which is significantly higher than the value determined for the earlier reported Fmoc-WWRR-NH$_2$ based hydrogel ($G' \sim 100$ Pa) and comparable to other previously reported polymer-based hydrogel wound dressings in literature.[38,39]

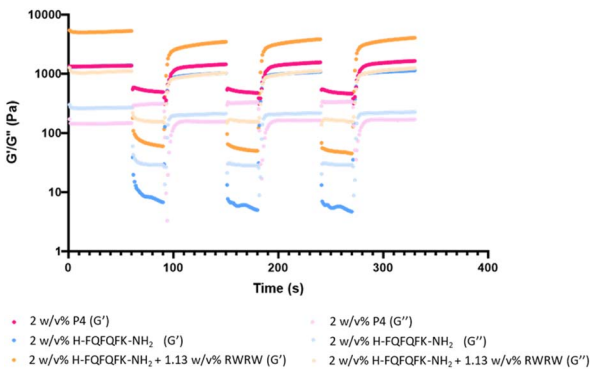

Fig. 4 Shear recovery experiment in which the storage modulus (G', darks shades) and loss modulus (G'', light shades) of 2 w/v% **P4** (pink), 2 w/v% **H-FQFQFK-NH$_2$** (blue) and 2 w/v% **H-FQFQFK-NH$_2$** +1.13 w/v% **H-RWRW-NH$_2$** (orange) are monitored over time. After 1 minute, the shear strain was increased from 1% to 50% for 30 seconds after which the shear strain was decreased back to 1%. The frequency did not change and equalled 1 Hz.

Furthermore, whereas the 2 w/v% **P4** biogel and the 2 w/v% **H-FQFQFK-NH$_2$** hydrogel are characterized by a similar G' (*ca.* 1300 Pa and *ca.* 1460 Pa), the G' of the gel consisting of 1.13 w/v% **H-RWRW-NH$_2$** encapsulated in 2 w/v% **H-FQFQFK-NH$_2$** is more than three times higher (*ca.* 4750 Pa). In a previous related study, it was also observed that encapsulation of a cargo resulted in an increase of G' from 400 Pa to 2500 Pa, depending on the type of cargo encapsulated within the hydrogel.[31] This indicates that the **H-RWRW-NH$_2$** peptide is dynamically interacting with the peptide fibres, resulting in a stronger hydrogel network. In addition, the shear recovery experiment demonstrates how the G' and G'' change upon increasing the oscillating shear strain (γ) from 1% to 50%. Noticeably, upon increasing γ, the G' (dark color in Fig. 4) and G'' (light color in Fig. 4) of both the co-formulation hydrogel (orange) and the **H-FQFQFK-NH$_2$** hydrogel (blue) significantly decrease. This occurs to the extent that the G'' value (*ca.* 160 Pa and 30 Pa) is now higher compared to the G' value (*ca* 67 Pa and *ca.* 8 Pa), accompanied by an increase in tan δ, indicating a transition from a hydrogel state to a flowing solution. Once the γ value decreased again (after 30 seconds) to 1%, the material rapidly returned to its original G' and G'' values, which is characteristic for non-covalent crosslinked networks and clearly demonstrates the shear-thinning behaviour as required for injectability.[40] The G' value of both hydrogel materials was not significantly affected after being deformed to their liquid state, illustrating the thixotropic nature of those gels. Whereas the **H-FQFQFK-NH$_2$** hydrogel and the co-formulation **H-FQFQFK-NH$_2$** hydrogel containing **H-RWRW-NH$_2$** became liquid upon increasing γ, this was not the case for the biogel **P4**. As can be seen from Fig. 4, the G'' value of the biogel is never higher than the G' value. When applying an increased γ, the G'' value increases to a value of *ca.* 309 Pa, whereas the G' value decreases to *ca.* 518 Pa. This results in a tan δ of 0.6, meaning that the material maintained its elastic properties upon deformation under the applied shear strain. Nonetheless, it was found that the **P4** hydrogel could be aspired and ejected through a needle, indicating injectability of the hydrogel. This observation indicates that the increase in γ during injection is likely higher than the 50% utilized during rheology. Indeed, the rheological strain sweep revealed that a strain higher than 500% was required to turn P4 hydrogel to viscoelastic liquid (Fig. SI13†).

Cytotoxicity

To determine whether the **H-FQFQFK-NH$_2$**, **H-RWRW-NH$_2$** and **P4** peptides exhibit any cytotoxicity, the metabolic activity of NIH/3T3 fibroblasts was monitored as a proxy for cell viability, using the XTT-proliferation assay. For this purpose, NIH/3T3 fibroblasts were incubated for 48 hours in a culture medium containing a final concentration of 0.25 mM of each peptide. Additionally, 100 μL of the **H-FQFQFK-NH$_2$** and **P4** hydrogel were deposited in the center of the wells of a 24 well plate. After 24 hours of incubation, Sytox green was added to each well to visualize the dead cells. The results are shown in Fig. 5.

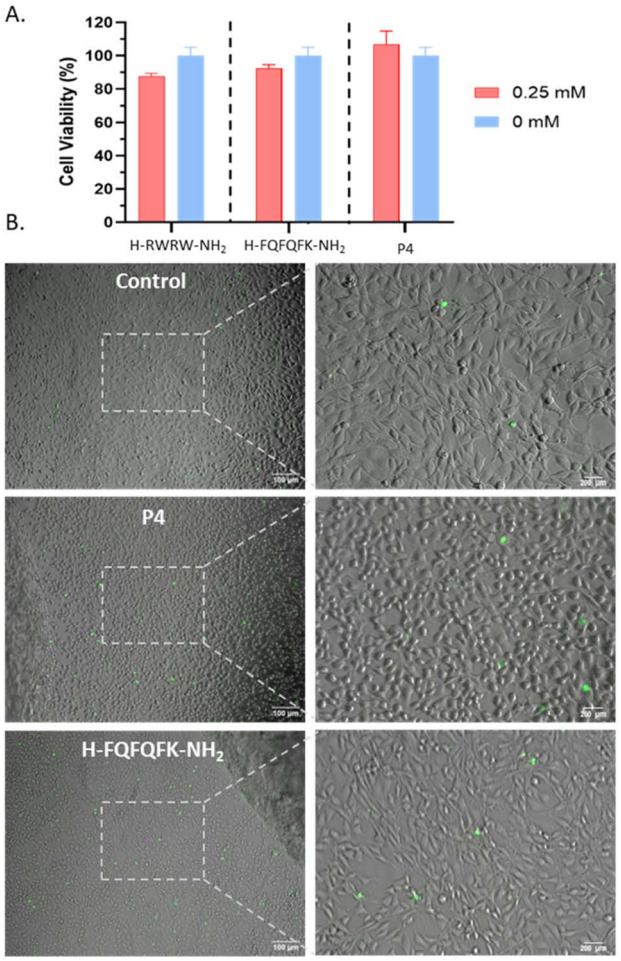

Fig. 5 (A) Representation of the cell viability (in%) after incubation of the NIH/3T3 fibroblasts with 250 μM of H-RWRW-NH_2, H-FQFQFK-NH_2 or P4 (red), compared to a control (blue). (B) Phase contrast and fluorescent images of NIH/3T3 cells incubated for 24 hours in medium (control), with 100 μL of 4 w/v% P4 biogel and a 2.46 w/v% H-FQFQFK-NH_2 hydrogel. The green spots represent dead cells. Each experiment was repeated three times.

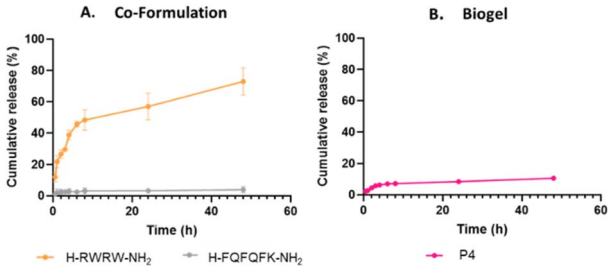

Fig. 6 Cumulative release (in%) as a function of time for (A) the co-formulation in which the release of both the H-FQFQFK-NH_2 (grey) and H-RWRW-NH_2 (orange) is followed and (B) the release of peptide P4 from its biogel. Each experiment was repeated three times.

As can be derived from Fig. 5A, incubation of NIH/3T3 fibroblasts with a 0.25 mM solution of **P4**, **H-FQFQFK-NH_2** or **H-RWRW-NH_2** peptide did not significantly affect cell viability. In addition, all hydrogel formulations were incubated with the NIH/3T3 fibroblasts for 24 hours in a 24 well plate. Phase contrast and fluorescent imaging showed no significant increase in dead cells upon comparing the control with the hydrogel formulations (Fig. 5B), indicating that the hydrogels as such do not show cytotoxic behavior under these conditions (Fig. SI11†).

In vitro release

Though an *in vitro* setting is not fully representative of the complex *in vivo* environment, it does allow evaluating the behaviour of the hydrogel formulations in more detail. By performing an *in vitro* release experiment, it can be assessed whether and how quickly the **H-RWRW-NH_2** peptide is released from the co-formulated hydrogel. Moreover, when looking at the release of the **P4** peptide, one can assess erosion of the **P4** hydrogels. In Fig. 6A, the release profile of the **H-RWRW-NH_2** peptide from the **H-FQFQFK-NH_2** hydrogel is presented, indicating a rapid burst release within the first hour (*ca.* 24%), followed by a more gradual and sustained release profile. From 24 hours until 48 hours, a slow release was still noted, resulting in 75% cargo release after 48 hours, while only 5% of the **H-FQFQFK-NH_2** hydrogelator itself was released. Furthermore, erosion of the **P4** peptide (Fig. 6B) from the biogel resulted in a peptide release of 10% after 48 hours, which is in the same range as the erosion observed for the **H-FQFQFK-NH_2** hydrogelator peptide.

In previous studies, focusing on the use of related peptide-based hydrogels as drug delivery vehicles in the context of painkilling applications, similar observations were made.[31] Depending on the type of encapsulated cargo, and its physico-chemical interactions within the hydrogel, almost complete *in vitro* release of cargo is observed after 48 hours. However, when these cargo-loaded hydrogel formulations were evaluated *in vivo*, data showed a much faster cargo release.[29] Additionally, the largest decrease in hydrogel volume, due to erosion of the peptide, was observed after 1 day.[29] Only 23% of the hydrogel volume remained 2 days post-injection. For that reason, it is anticipated that even though the *in vitro* release data show that only 10% of the **P4** biogelator is being released after 48 hours, one can expect a significantly higher release *in vivo*. Given these discrepancies between *in vitro* and *in vivo* release, it is further difficult to anticipate what the exact release profile will be upon topical administration. Therefore, a more representative assay based on an *in vitro* wound model was performed.

In vitro wound model assay

To assess the potential of the co-formulated gel and the **P4** biogel for biofilm destruction and topical wound healing applications, an *in vitro* wound model assay was carried out on three different bacteria: *S. aureus*, *P. aeruginosa* and *A. baumannii*. For this purpose, an artificial dermis (AD) was prepared as a substrate for biofilm formation.[41] The artificial dermis is composed of an upper layer consisting of a chemically cross-linked hyaluronic acid (HA) spongy sheet while the lower layer is a spongy sheet composed of HA and collagen (see ESI† section 6.1 for preparation details).

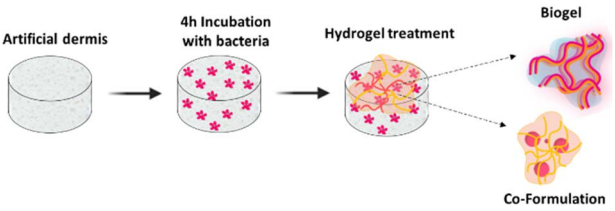

Fig. 7 Experimental set-up of the *in vitro* biofilm model for chronic wound infection. First, a solution of bacteria is incubated for 4 hours on top of the artificial dermis. Subsequently, a hydrogel (biogel or co-formulated gel) is applied on top of the dermis.

The experiment was performed in an eradication set-up, where bacteria were allowed to actively spread over the AD surface for 4 hours prior to treatment (see ESI† section 6.2 for more details). Subsequently, 200 μL of the hydrogel formulation was administered on top of the AD. After 20 hours of incubation, the number of colony forming units per dermis was determined by plating the AD containing suspensions (see ESI† section 6.3 for more details). An illustration of the experimental set-up is given in Fig. 7.

For this experiment, rather than ensuring identical w/v% composition, we made sure that the molar concentration of each peptide that was incorporated in the different hydrogels, was the same so that different outcomes of the experiment are solely due to different antibacterial properties and release profiles between the peptide hydrogels. Therefore, the co-formulated hydrogel was composed of 1.23 w/v% **H-FQFQFK-NH$_2$** + 1.14 w/v% **H-RWRW-NH$_2$**, the biogel was composed of 2 w/v% of **P4**, and the 1.23 w/v% **H-FQFQFK-NH$_2$** hydrogel served as a control. As an additional control, administration of a 1.14 w/v% **H-RWRW-NH$_2$** solution to the AD was also included. The results are shown in Fig. 8. A Shapiro–Wilk test was performed indicating that the data set was normally distributed and a one-way anova test could be applied to determine the significance ($P < 0.05$) of the results. From the one way anova test, it could be derived that in case of *S. aureus*, only for the **H-RWRW-NH$_2$** peptide solution (****) and co-formulation hydrogel (**) the number of CFU recovered per dermis differed significantly from the CFU per dermis obtained from an untreated dermis. As expected, no significant effect was observed by mere treatment with **H-FQFQFK-NH$_2$** hydrogel. In case the dermis was treated with the **H-RWRW-NH$_2$** peptide solution, no surviving bacteria remained, and after treatment with the co-formulation, only 2.9% of bacteria survived the treatment. Treatment of the dermis with the **P4** biogel resulted in 28.2% of remaining bacteria which is not considered significantly lower compared to the untreated dermis, which can be related to the too slow release of the peptide from the hydrogel to reach the MBC.

Remaining amount of bacteria (%)			
	S. aureus	*A. baumannii*	*P. aeruginosa*
Untreated	100	100	100
P4	5.3	0.4	14.1
H-FQFQFK-NH$_2$	28.2	84	69.9
H-RWRW-NH$_2$	0	10^{-4}	3.9×10^{-4}
H-FQFQFK-NH$_2$ + H-RWRW-NH$_2$	2.9	0.1	6.8

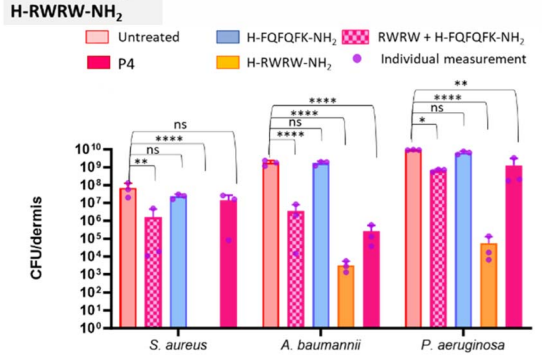

Fig. 8 The number of colony forming units (CFU) per dermis of *S. aureus*, *A. baumanni* or *P. aeruginosa*, obtained after 20 hours of treatment with either the co-formulated hydrogel (pink squares) composed of 1.23 w/v% H-FQFQFK-NH$_2$ + 1.14 w/v% H-RWRW-NH$_2$, the biogel made from 2 w/v% P4 (pink), a 1.23 w/v% H-FQFQFK-NH$_2$ hydrogel (blue) or a 1.14 w/v% solution of H-RWRW-NH$_2$ (orange). When no treatment was applied, the CFU per dermis are represented by the red bars. Data points presenting mean values ± SD ($n = 3$): (*) $P < 0.05$, (**) $P < 0.01$, (***) $P < 0.001$, (****) $P < 0.0001$.

In case the dermis was infected with *A. baumannii* or *P. aeruginosa*, again and as expected, treatment of the dermis with the parent hydrogelator **H-FQFQFK-NH$_2$** only did not result in a significant difference with respect to the untreated situation. In case the **H-FQFQFK-NH$_2$** co-formulation with **H-RWRW-NH$_2$** was applied to the *A. baumannii* infected dermis, 0.1% of the bacteria remained whereas addition of the **H-RWRW-NH$_2$** peptide solution resulted in 10^{-4}% of remaining bacteria in the dermis. In this case, when the **P4** biogel was applied on top of the dermis, only 0.4% of bacteria remained after 20 hours. In the case of the *P. aeruginosa* infected dermis, upon treatment with the co-formulation 6.8% of bacteria remained whereas with the **H-RWRW-NH$_2$** solution, only 3.9×10^{-4}% of the bacteria remained. Treatment with the **P4** biogel resulted in 14.1% of remaining bacteria.

Altogether, the biogel and the co-formulated gel containing the **H-RWRW-NH$_2$** peptide embedded in **H-FQFQFK-NH$_2$** demonstrate pronounced antibacterial activity, especially in the case of *A. baumannii* albeit not to the same extent as the **H-RWRW-NH$_2$** peptide in solution. In this artificial dermis model, practically, effects can only be measured over a limited period and the amount of antibacterial **H-RWRW-NH$_2$** or **P4** released from the hydrogel after 20 hours might not seem competitive when compared to application of the **H-RWRW-NH$_2$** peptide in solution. However, a prolonged antibacterial effect can be expected for topical administration of the hydrogel formulations when compared to application of an **H-RWRW-NH$_2$** solution. Furthermore, addition of such hydrogel formulations on top of a biofilm-covered surface, is operationally simpler than administering a **H-RWRW-NH$_2$** solution. Mixing-in the free **H-RWRW-NH$_2$** peptide in a **P4** biogel might further enhance potency of the antibacterial formulation.

Conclusions

In the current work, an antibacterial hydrogel was obtained by covalently merging the short antibacterial peptide **H-RWRW-NH$_2$**

with a short hydrogelating peptide sequence **H-FQFQFK-NH_2**. The resulting biogel (**P4**) as well as the co-formulation alternative containing the antimicrobial tetrapeptide **H-RWRW-NH_2** in the parent hydrogelator matrix were evaluated by means of antibacterial assays, cytotoxicity assays and an *in vitro* wound model experiment. In contrast to the recently reported Fmoc-WWRR-NH_2 hydrogel system,[19] encompassing a related shorter but N-terminally protected sequence, our antibacterial hydrogel is longer but composed of natural amino acids only, without any further unnatural moieties required for self-assembly. The latter represents a significant advantage as it has been earlier shown that Fmoc-containing gelators can become necrotic to some human cell lines over longer incubation periods due to byproducts of Fmoc degradation.[42,43] In addition, compared to the Fmoc-WWRR-NH_2 system, both the **P4** biogel and the co-formulation of **H-RWRW-NH_2** within the **H-FQFQFK-NH_2** hydrogel are characterised by better mechanical properties and a lower w/v% of peptide hydrogelator is needed to obtain hydrogels. The obtained data demonstrate that both the biogel **P4** and the **H-FQFQFK-NH_2** hydrogel co-formulated with **H-RWRW-NH_2** show great potential to be used in wound healing or biofilm destruction applications. Both hydrogel formulations appeared effective in killing *A. baumannii* present in an artificial dermis. After 20 hours of treatment with the hydrogel formulation, 0.4% of bacteria remained in case of the **P4** biogel, whereas 0.1% of bacteria remained upon treatment with the co-formulation. Both hydrogels are thixotropic, rendering administration of these gels on top of wounds or surfaces simple.

Data availability

The data supporting this article have been included as part of the ESI.†

Author contributions

The authors confirm contribution to the paper as follows: D. A. synthesized all peptides, performed rheology and assisted with the cytotoxicity assays. D. A. also wrote the manuscript draft and processed the data. A. T. performed the XTT assay and contributed to the writing. H. V. performed the CD measurements, the ThT assay, the rheological temperature ramp experiment, and contributed to the writing. P. R. performed all antibacterial assays. M. V. T supervised the cytotoxicity experiments. A. M., S. B., C. M., R. H. and T. C. coordinated the study and contributed to the final version of the manuscript. All authors reviewed the results and approved the final version of the manuscript.

Conflicts of interest

There are no conflicts to declare.

Acknowledgements

DA is indebted to the FWO-Vlaanderen for a PhD grant. AT is indebted to the FWO-Vlaanderen for a position as postdoctoral researcher. S. B. and C. M. acknowledge the Research Council of the Vrije Universiteit Brussel (VUB) for financial support through the SRP50 program. C. M., R. H. and S. B. additionally thank the Scientific Research Network (Wetenschappelijke Onderzoeksgemeenschap) "Supramolecular Chemistry and Materials" of the Research Foundation Flanders (FWO) for financial support. The Research Foundation Flanders (FWO) is further thanked for financial support through project G.0541.19N. The authors thank Fatma Nalan Çetin and the group of polymer chemistry & biomaterials of Ghent University for technical assistance in obtaining rheological data.

Notes and references

1 A. Cassini, L. D. Högberg, D. Plachouras, A. Quattrocchi, A. Hoxha, G. S. Simonsen, M. Colomb-Cotinat, M. E. Kretzschmar, B. Devleesschauwer, M. Cecchini, D. A. Ouakrim, T. C. Oliveira, M. J. Struelens, C. Suetens, D. L. Monnet, R. Strauss, K. Mertens, T. Struyf, B. Catry, K. Latour, I. N. Ivanov, E. G. Dobreva, A. T. Andraševic, S. Soprek, A. Budimir, N. Paphitou, H. Žemlicková, S. S. Olsen, U. W. Sönksen, P. Märtin, M. Ivanova, O. Lyytikäinen, J. Jalava, B. Coignard, T. Eckmanns, M. A. Sin, S. Haller, G. L. Daikos, A. Gikas, S. Tsiodras, F. Kontopidou, Á. Tóth, Á. Hajdu, Ó. Guólaugsson, K. G. Kristinsson, S. Murchan, K. Burns, P. Pezzotti, C. Gagliotti, U. Dumpis, A. Liuimiene, M. Perrin, M. A. Borg, S. C. de Greeff, J. C. Monen, M. B. Koek, P. Elstrøm, D. Zabicka, A. Deptula, W. Hryniewicz, M. Caniça, P. J. Nogueira, P. A. Fernandes, V. Manageiro, G. A. Popescu, R. I. Serban, E. Schréterová, S. Litvová, M. Štefkovicová, J. Kolman, I. Klavs, A. Korošec, B. Aracil, A. Asensio, M. Pérez-Vázquez, H. Billström, S. Larsson, J. S. Reilly, A. Johnson and S. Hopkins, *Lancet Infect. Dis.*, 2019, **19**, 56–66.
2 Z. Khatoon, C. D. McTiernan, E. J. Suuronen, T. F. Mah and E. I. Alarcon, *Heliyon*, 2018, **4**, e01067.
3 M. Malone, T. Bjarnsholt, A. j. McBain, G. a. James, P. Stoodley, D. Leaper, M. Tachi, G. Schultz, T. Swanson, R. D. Wolcott and J. Wound, *Care*, 2017, **26**, 20–25.
4 C. A. Fleck, *J. Am. Col. Certif. Wound. Spec.*, 2009, **1**, 109–113.
5 A. J. Wodash, *J. Am. Col. Certif. Wound. Spec.*, 2012, **4**, 63–66.
6 J. Liu, W. Jiang, Y. Xu Q and Y. Zheng, *Gels*, 2022, **8**, 503.
7 X. Zhang, M. Qin, M. Xu, F. Miao, C. Merzougui, X. Zhang, Y. Wei, W. Chen and D. Huang, *Eur. Polym. J.*, 2021, **146**, 110268.
8 T. Xu, Y. Tian, R. Zhang, B. Yu, H. Cong and Y. Shen, *Appl. Mater. Today*, 2021, **25**, 101224.
9 R. Binaymotlagh, A. Del Giudice, S. Mignardi, F. Amato, A. G. Marrani, F. Sivori, I. Cavallo, E. G. Di Domenico, C. Palocci and L. Chronopoulou, *Gels*, 2022, **8**, 700.
10 M. Criado-Gonzalez, M. H. Iqbal, A. Carvalho, M. Schmutz, L. Jierry, P. Schaaf and F. Boulmedais, *Front. Bioeng. Biotechnol.*, 2020, **8**, 938.
11 Y. Guo, S. Wang, H. Du, X. Chen and H. Fei, *Biomacromolecules*, 2019, **20**, 558–565.

12 L. Yang, C. Zhang, F. Huang, J. Liu, Y. Zhang, C. Yang, C. Ren, L. Chu, B. Liu and J. Liu, *J. Controlled Release*, 2020, **324**, 354–365.
13 J. Li, R. Xing, S. Bai and X. Yan, *Soft Matter*, 2019, **15**, 1704–1715.
14 A. Adak, S. Ghosh, V. Gupta and S. Ghosh, *Biomacromolecules*, 2019, **20**, 1889–1898.
15 M. A. Paduszynska, M. Maciejewska, D. Neubauer, K. Golacki, M. Szymukowicz, M. Bauer and W. Kamysz, *Pharmaceutics*, 2019, **11**, 506.
16 R. Sharma, S. Tomar, S. Puri and N. Wangoo, *Chem. Bio. Chem.*, 2022, **23**, e202200499.
17 Y. Zhao, X. Du, L. Jiang, H. Luo, F. Wang, J. Wang, L. Qiu, L. Liu, X. Liu, X. Wang, P. Jiang and J. Wang, *J. Nanosci. Nanotechnol.*, 2020, **20**, 2087–2094.
18 Z. Guo, Y. Wang, T. Tan, Y. Ji, J. Hu and Y. Zhang, *ACS Biomater. Sci. Eng.*, 2021, **7**, 1703–1712.
19 P. Cardoso, S. Appiah Danso, A. Hung, C. Dekiwadia, N. Pradhan, J. Strachan, B. McDonald, K. Firipis, J. F. White, A. Aburto-Medina, C. E. Conn and C. Valéry, *Front. Chem.*, 2023, **10**, 1009468.
20 P. Cardoso, H. Glossop, T. G. Meikle, A. Aburto-Medina, C. E. Conn, V. Sarojini and C. Valery, *Biophys. Rev.*, 2021, **13**, 35–69.
21 M. C. Branco, D. J. Pochan, N. J. Wagner and J. P. Schneider, *Biomaterials*, 2009, **30**, 1339–1347.
22 J. K. Kretsinger, L. A. Haines, B. Ozbas, D. J. Pochan and J. P. Schneider, *Biomaterials*, 2005, **26**, 5177–5186.
23 D. A. Salick, J. K. Kretsinger, D. J. Pochan and J. P. Schneider, *J. Am. Chem. Soc.*, 2007, **129**, 14793–14799.
24 D. A. Salick, D. J. Pochan and J. P. Schneider, *Adv. Mater.*, 2009, **21**, 4120–4123.
25 Z. Azoulay, P. Aibinder, A. Gancz, J. Moran-Gilad, S. Navon-Venezia and H. Rapaport, *Acta Biomater.*, 2021, **125**, 231–241.
26 J. Zhou, R. Cha, Z. Wu, C. Zhang, Y. He, H. Zhang, K. Liu, M. S. Fareed, Z. Wang, C. Yang, Y. Zhang, W. Yan and K. Wang, *Nano Today*, 2023, **49**, 101801.
27 M. Bibian, J. Mangelschots, J. Gardiner, L. Waddington, M. M. Diaz Acevedo, B. G. De Geest, B. Van Mele, A. Madder, R. Hoogenboom and S. Ballet, *J. Mater. Chem. B*, 2015, **3**, 759–765.
28 C. Martin, M. Dumitrascuta, M. Mannes, A. Lantero, D. Bucher, K. Walker, Y. Van Wanseele, E. Oyen, S. Hernot, A. Van Eeckhaut, A. Madder, R. Hoogenboom, M. Spetea and S. Ballet, *J. Med. Chem.*, 2018, **61**, 9784–9789.
29 E. Oyen, C. Martin, V. Caveliers, A. Madder, B. Van Mele, R. Hoogenboom, S. Hernot and S. Ballet, *Biomacromolecules*, 2017, **18**, 994–1001.
30 C. Martin, E. Oyen, J. Mangelschots, M. Bibian, T. Ben Haddou, J. Andrade, J. Gardiner, B. Van Mele, A. Madder, R. Hoogenboom, M. Spetea and S. Ballet, *MedChemComm*, 2016, **7**, 542–549.
31 J. Heremans, L. Chevillard, M. Mannes, J. Mangialetto, K. Leroy, J. F. White, A. Lamouroux, M. Vinken, J. Gardiner, B. Van Mele, N. Van den Brande, R. Hoogenboom, A. Madder, V. Caveliers, B. Mégarbane, S. Hernot, S. Ballet and C. Martin, *J. Controlled Release*, 2022, **350**, 514–524.
32 Z. Liu, A. Brady, A. Young, B. Rasimick, K. Chen, C. Zhou and N. R. Kallenbach, *Antimicrob. Agents Chemother.*, 2007, **51**, 597–603.
33 S. Ramesh, T. Govender, H. G. Kruger, B. G. de la Torre and F. Albericio, *J. Pept. Sci.*, 2016, **22**, 438–451.
34 Z. Liu, H. Deshazer, A. J. Rice, K. Chen, C. Zhou and N. R. Kallenbach, *J. Med. Chem.*, 2006, **49**, 3436–3439.
35 T. De Maeseneer, T. Cauwenbergh, J. Gardiner, J. F. White, W. Thielemans, C. Martin, P. Moldenaers, S. Ballet and R. Cardinaels, *Macromol. Biosci.*, 2024, **24**, 2300579.
36 D. Andersson, U. Carlsson and P. O. Freskgård, *Eur. J. Biochem.*, 2001, **268**, 1118–1128.
37 G. Stojkov, Z. Niyazov, F. Picchioni and R. K. Bose, *Gels*, 2021, **7**, 255.
38 W. Huang, Y. Wang, Z. Huang, X. Wang, L. Chen, Y. Zhang and L. Zhang, *ACS Appl. Mater. Interfaces*, 2018, **10**, 41076–41088.
39 T. Guan, J. Li, C. Chen and Y. Liu, *Adv. Sci.*, 2022, **9**, 2104165.
40 L. M. Stapleton, A. N. Steele, H. Wang, H. Lopez Hernandez, A. C. Yu, M. J. Paulsen, A. A. A. Smith, G. A. Roth, A. D. Thakore, H. J. Lucian, K. P. Totherow, S. W. Baker, Y. Tada, J. M. Farry, A. Eskandari, C. E. Hironaka, K. J. Jaatinen, K. M. Williams, H. Bergamasco, C. Marschel, B. Chadwick, F. Grady, M. Ma, E. A. Appel and Y. J. Woo, *Nat. Biomed. Eng.*, 2019, **3**, 611–620.
41 G. Brackman, M. J. Garcia-Fernandez, J. Lenoir, L. De Meyer, J.-P. Remon, T. De Beer, A. Concheiro, C. Alvarez-Lorenzo and T. Coenye, *Macromol. Biosci.*, 2016, **16**, 859–869.
42 B. L. Abraham, W. Liyanage and B. L. Nilsson, *Langmuir*, 2019, **35**, 14939–14948.
43 W. Ty Truong, Y. Su, D. Gloria, F. Braet and P. Thordarson, *Biomater. Sci.*, 2015, **3**, 298–307.